High Rate Discharge Performance and Thermal Stability of Heat-Treated Carbon Nanobeads

Sano, Atsushi; Kurihara, Masato; Abe, Takeshi; Ogumi, Zempachi

Journal of The Electrochemical Society, **156** (8) A682-A687 (2009)
0013-4651/2009/156(8)/A682/6/$25.00 © The Electrochemical Society

High Rate Discharge Performance and Thermal Stability of Heat-Treated Carbon Nanobeads

Atsushi Sano,[a,*,z] Masato Kurihara,[a,*] Takeshi Abe,[b] and Zempachi Ogumi[b,]**

[a]*TDK Corporation, Devices Development Center, Chiba 286-8588, Japan*
[b]*Department of Energy and Hydrocarbon Chemistry, Graduate School of Engineering, Kyoto University, Kyoto 615-8510, Japan*

The electrochemical characteristics of carbon nanobeads (CNBs) heat-treated at 1000, 1500, 2000, and 2800°C were investigated. The discharge capacity was highest at the high rate (>10 C) in the 2000°C heat-treated CNBs. Electrochemical impedance spectrometry indicated that the charge-transfer resistance of 2000°C heat-treated CNBs was smaller, over a wide potential range, than for 1500 and 2800°C CNBs. From the differential scanning calorimetry measurement, the temperature of CNBs heat-treatment had a direct linear relationship to the temperature of the largest exothermic peak: 2800 < 2000 < 1500 < 1000°C. The heat value of the large exothermic peak was proportional to the energy of lithiated CNBs.
 [DOI: 10.1149/1.3141523]

Manuscript submitted February 23, 2009; revised manuscript received April 30, 2009. Published June 4, 2009.

With the commercialization of lithium-ion batteries, these batteries, taking advantage of higher energy density than other batteries, are now being used as power sources for portable devices. Recently, lithium-ion batteries have attracted attention as energy storage devices for load leveling or a hybrid energy conversion systems, e.g., for leveling of wind-mill generation or hybrid electric vehicle. To satisfy the demands of these applications, a high rate charge and discharge performance is required. These applications need large input current and large output current because input and output power varies rapidly. But the high rate ability of lithium-ion batteries is inferior to Ni–Cd or Ni–MH batteries.

One of the key factors influencing rapid charge/discharge is the carbon negative electrode. Graphite has been used extensively as a negative electrode. The graphite electrode has many advantages such as flat potentials as low as Li metal, small volume expansion, and high reversibility of lithium-ion intercalation and deintercalation. However, lithium-ion diffusion in graphite can be the rate-determining step in intercalation or deintercalation.[1,2] Therefore increasing specific lithium-ion diffusion in the carbon negative electrode is important to the improvement of rapid charge/discharge performance.

To increase the specific diffusion rate, small size carbonaceous materials have been studied. Grinding graphite,[3,4] carbon nanotubes,[5,6] mesoporous carbon,[7,8] nanosized hard carbon spherules,[9] and graphitized nanocarbon bead[10] were all studied for use as high rate negative electrodes. Particle size dependence of high rate performance was investigated by Buqa et al.[11] The small particle graphite SFG6 showed higher rate capability than large size graphite SFG44. They concluded that the difference was due to the length of the diffusion path in the electrode.

Markovsky et al.[12] reported on the lithium-ion diffusion coefficients of different sized graphite particles. The diffusion coefficient was studied using potentiostatic intermittent titration technique.[13,14] Their results showed that the smaller particle size had the smaller diffusion coefficient. They reported that the surface film which forms a rigid matrix interferes with volume expansion during intercalation and the effect is pronounced at small size particle.

The thermal stability of electrodes was studied extensively by the method of differential scanning calorimetry (DSC)[15-18] and accelerated rate calorimetry.[19] Du Pasquier et al. studied thermal reaction of negative electrodes. They reported that a breakdown of solid electrolyte interphase (SEI) took place at 120–140°C followed by the reaction of lithiated graphite with the melted binder above 300°C.[15] Heat generation between 120 and 180°C strongly depends on the Brunauer, Emmett, and Teller (BET) surface area of the graphite electrodes and heat generation between 280 and 400°C is strongly affected by the degree of lithiation of the negative electrode. Maleki et al. also reported that the total heat generation in the negative electrode increases with increasing lithiation, as determined by a DSC measurement. The chemical reaction temperature of lithiated graphite was not changed by the degree of lithiation. However increasing lithiation of hard carbon lowered the reaction temperature of lithiated hard carbon.

Physical characteristics of heat-treated petroleum coke and mesocarbon microbeads were extensively studied by Dahn et al.[20,21] and Tatsumi et al.[22] They reported on an X-ray diffraction (XRD) study of graphitized carbon and disorder carbon and several types of hard carbons. They reported that there is no evidence for the formation of staged phases in intercalated coke heated below 2100°C, while 2200°C treated coke showed a dx/dV feature corresponding to the coexistence of different stage phases. They suggested that there is a relationship between disorder probability and reversible capacity and that 2000°C treated coke had the lowest reversible capacity among heat-treated soft carbons.

In this study, we investigated the high rate charge/discharge characteristics of carbon nanobeads (CNBs) which were heat-treated from 1000 to 2800°C. We focused on the relationship between the high rate performance and the temperature of heat-treatment of the nanocarbon. The physical properties were investigated by scanning electron microscope, XRD, Raman scattering spectroscopy, X-ray photoelectron spectroscopy (XPS), hydrogen and oxygen analysis, BET surface area measurement, and pore size distribution. The high rate charge/discharge characteristics were investigated using several type cells with different counter electrodes. $LiNi_{1/3}Mn_{1/3}Co_{1/3}O_2$ and $LiFePO_4$ were used as the counter electrodes. Electrochemical impedance spectrometry (EIS) was also studied.

Based on these results, the performance of heat-treated CNBs will be discussed.

Experimental

CNBs were prepared by chemical vapor deposition at Tokai Carbon Co. Ltd. The detailed preparation procedure was previously reported.[10,23] CNBs were heat-treated in an electric oven under Ar atmosphere at 1200, 1500, 2000, and 2800°C. The temperature was maintained for 20 h.

Powder XRD measurements were made using Rigaku Rint2500 equipped with Cu target and a diffracted beam monochromator. The receiving slit was 0.8 mm. The average crystallite sizes along the crystallographic c-axis direction (Lc) and the a-axis direction (La) were determined from the full width at half-maximum of carbon (002) and (100) Bragg diffraction reflexes.

The scanning electron microscopy (SEM) images were recorded with a SEM JEOL JSM-6340F. XPS was performed on a Shimadzu AXIS-HSX. Raman scattering spectroscopy was measured with

* Electrochemical Society Active Member.
** Electrochemical Society Fellow.
z E-mail: sanoa@jp.tdk.com

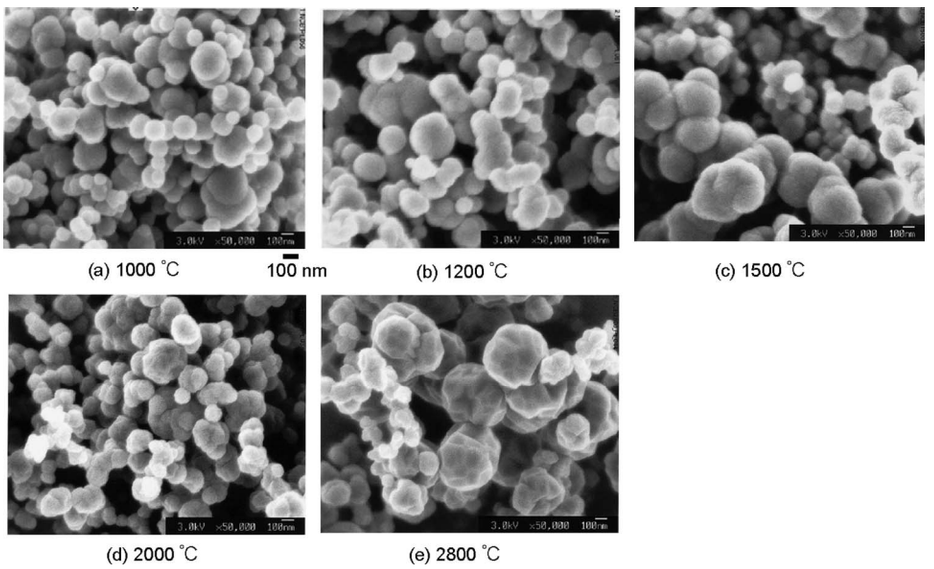

Figure 1. SEM images of heat-treated CNBs at (a) 1000, (b) 1200, (c) 1500, (d) 2000, and (e) 2800°C.

Horiba LabRAM using a 514.5 nm Ar laser. Oxygen and hydrogen were measured with Leco TC-600. We used the N_2 absorption method (Nova 1200, Yuasa Ionics) to measure the BET surface area and pore size distribution.

Charge and discharge measurements.— Negative electrodes were made by coating slurries with a doctor blade method. Ninety wt % CNBs or heat-treated CNBs and 2 wt % acetylene black (Denki Kagaku Kogyo) and 8 wt % poly(vinylidene fluoride) (Kureha Kagaku) were mixed and added to 1-methyl-2-pyrrolidinone (NMP). The mixture was stirred and NMP was added until the mixture became a slurry. The slurry was coated on copper foil (18 μm) dried at 110°C, and pressed by a roll press. The density of the electrodes was adjusted to about 1.4 g cm^{-3}. An electrode punched out to 12 mm in diameter was used as the working electrode.

To measure charge/discharge characteristics, a three-electrode cell was used. The counter and reference electrodes were lithium foil. One mol dm^{-3} $LiPF_6$ dissolved in ethylene carbonate + diethyl carbonate (EC + DEC) (3:7 volume ratio) was used as the electrolyte.

We used $LiNi_{1/3}Mn_{1/3}Co_{1/3}O_2$ or $LiFePO_4$ as the counter electrode to evaluate the cell performance. The cell consisted of aluminum-laminated film as a package. Charge and discharge measurement was carried out with Hokuto Denko HJ. Constant current charge and discharge was used at various current densities. The cutoff voltage was over the range of 0.005–3.0 V.

EIS was measured with a Solartron 1260 frequency response analyzer coupled with a Solartron 1287 electrochemical interface. The electrode potential was stepped from an open-circuit potential to a certain potential. After sufficient time, the impedance was measured by applying a sine wave of 5 mV amplitude over the frequency range from 100 kHz to 10 MHz.

DSC was carried out by Rigaku Thermo Plus DSC8320. Charged electrodes were scraped from the current collector and put into a pressure-resistant special use stainless steel pan under Ar atmosphere.

Results

Figure 1 shows SEM images of heat-treated CNBs. Between 1000 and 1200°C there is not much difference. Spherical shapes began to change to polyhedron shapes on going from 1200 to 1500°C. At 2000°C the basal plane was partially observed. An almost perfect polyhedron shape was formed at 2800°C.

The parameters analyzed by XRD are shown in Table I. Yamaki et al. reported that $d(002)$ of petroleum cokes treated at 2800°C was 0.3352 nm.[18] The lattice spacing of CNBs heat-treated at 2800°C was 0.339 nm. The difference in raw material might affect the crystallinity of heat-treated carbonaceous materials.[18-20]

Lc increased significantly between 1500 and 2000°C, and *La* increased significantly between 2000 and 2800°C. This result shows that the crystal first grew along the *c*-axis direction and then along the *a*-axis direction. The crystalline growth progressed anisotropically.

Figure 2 shows the Raman spectra of heat-treated CNBs. The peak at 1580 cm^{-1} (G band) represents the graphite structure. The G band was more pronounced for CNBs treated at 2000 and 2800°C than under 1500°C.

Table I. XRD parameters of heat-treated CNBs.

	1000°C	1200°C	1500°C	2000°C	2800°C
$d(002)$ (Å)	3.60	3.55	3.46	3.44	3.39
La (Å)	46	20	29	82	207
Lc (Å)	30	23	42	128	140

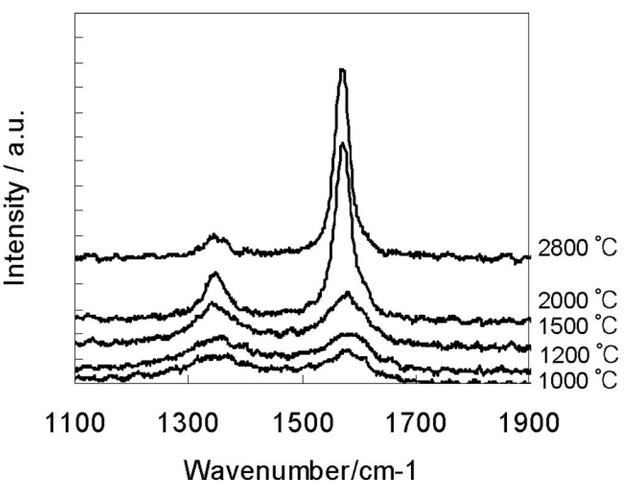

Figure 2. Raman spectra of the heat-treated CNB electrode.

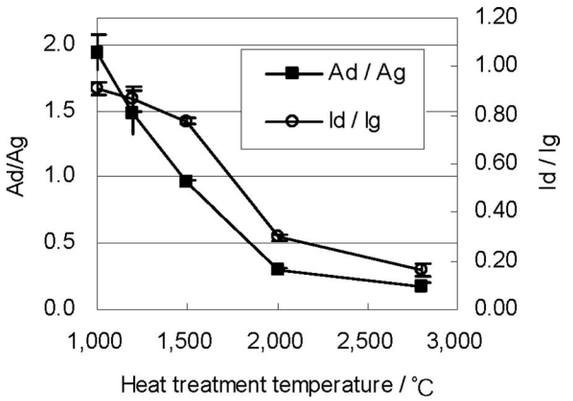

Figure 3. R value (I_d/I_g and A_d/A_g) of the heat-treated CNB electrode.

Figure 3 shows the R value ($I_{1360\ cm^{-1}(d)}/I_{1580\ cm^{-1}(g)}$) which represents the degree of disorder of the graphite structure. I_d/I_g is significantly different between 1500 and 2000°C. The peak area ratio ($A_{1360\ cm^{-1}(d)}/A_{1580\ cm^{-1}(g)}$) shows the same trend. There is a significant difference between 1500 and 2000°C. The results of the R value indicate that the graphitization developed as the temperature increases to 2000°C. Above 2000°C it did not develop significantly.

The Raman spectrometry contains baseline intensity (background). The intensity of the baseline reflects the intensity of carbon

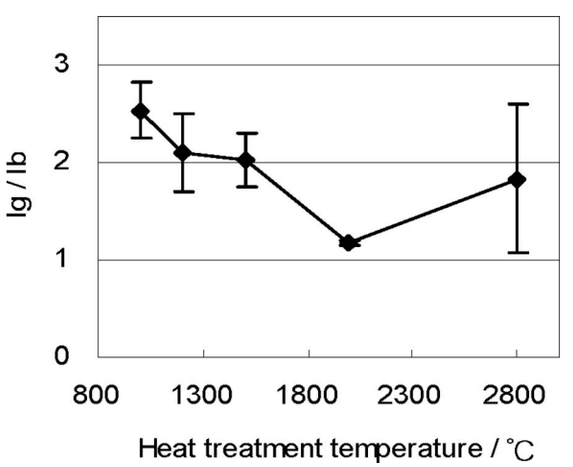

Figure 4. I_g/I_b value of the heat-treated CNB electrode.

Table II. The amount of hydrogen and oxygen and BET surface area of heat-treated CNBs.

	1000°C	1200°C	1500°C	2000°C	2800°C
O (%)	0.070	0.019	0.017	0.004	0.005
H (%)	0.36	0.11	0.013	0.0001	0.0004
BET ($m^2\ g^{-1}$)	15.3	14.6	15.7	14.4	14.4

fluorescence.[24] To specify the effect of carbon fluorescence, the I_b value was used. The I_b value is calculated from Fig. 3, I_b = (peak intensity at 1580 cm^{-1})-(extrapolated baseline), while I_g = (peak intensity at 1580 cm^{-1}). The ratio of I_g to I_b (I_g/I_b) is shown in Fig. 4. I_g/I_b was lowest for CNBs treated at 2000°C. I_b for CNBs treated at 2800°C is larger than that of 2000°C. Carbon fluorescence comes from the nongraphitized region.[24] This suggests that CNBs treated at 2000°C contains the smallest disordered phase which causes fluorescence.

Table II shows the results of hydrogen and oxygen analysis by combustion method. The amount of oxygen decreased significantly between 1500 and 2000°C. The 2000 and 2800°C are not much different regarding the amount of oxygen within experimental accuracy.

The amount of hydrogen was decreased by about one-tenth between 1200 and 1500°C. From 1500 to 2000°C, the amount of hydrogen decreased by about one-hundredth.

The results of BET surface area measurements are shown in Table II. The BET surface area of heat-treated CNBs was almost the same at each temperature. The evenness of the BET surface area among samples is important in comparing the heat-treatment effect because the electrochemical properties are strongly dependent on the surface area. Heat-treatment also does not make a significant difference in the pore size distribution analyzed by the N_2 absorption method.

Figure 5 shows the charge/discharge curves of the first and second cycles for each of the heat-treated CNBs. As the temperature of heat-treatment increased, the average charge/discharge potential decreased. The reversible capacity was minimum in 2000°C. The capacity of 2800°C was higher than for 2000°C. This tendency was like petroleum cokes, and mesocarbon pitch has been studied by many researchers.[18-20]

The plateau appears at 0.8 V in 2800°C CNBs. This plateau most likely shows the decomposition of the electrolyte, which is observed among graphite negative electrodes.[25] Besenhard et al. reported that a peak at 0.8 V observed by cyclic voltammmetry was due to film formation and solvated lithium ion intercalated into graphite forming graphite intercalation compounds (GICs) at those potentials.[25] Thus the plateau observed at 0.8 V would be specific for graphitized

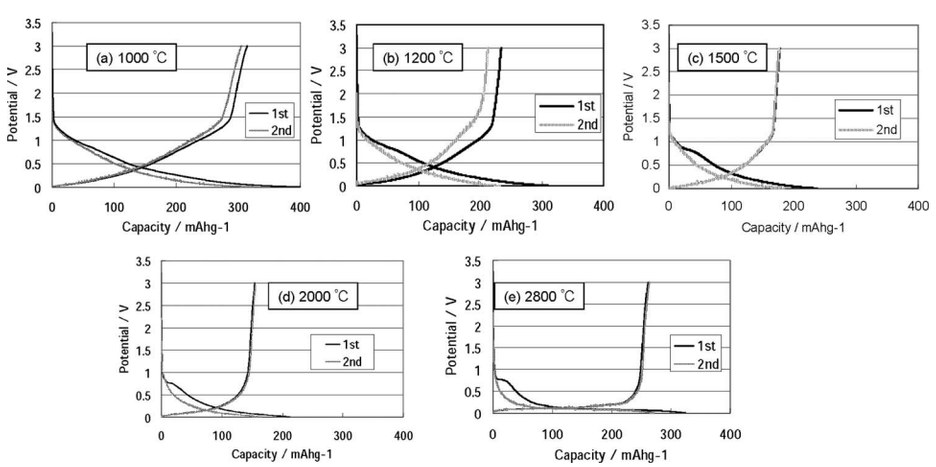

Figure 5. Charge and discharge curves of heat-treated CNBs at (a) 1000, (b) 1200, (c) 1500, (d) 2000, and (e) 2800°C.

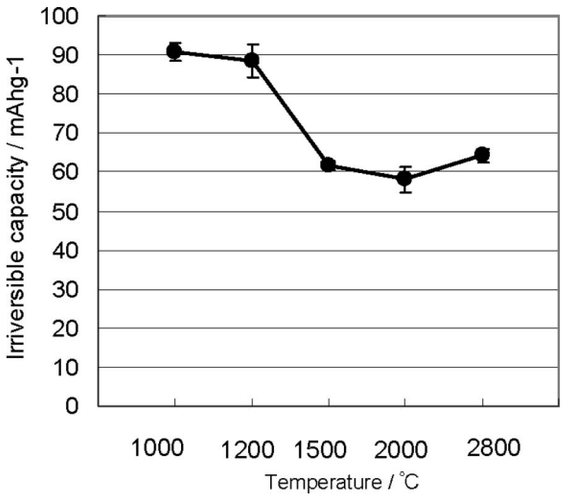

Figure 6. Irreversible capacity of heat-treated CNBs at first cycle.

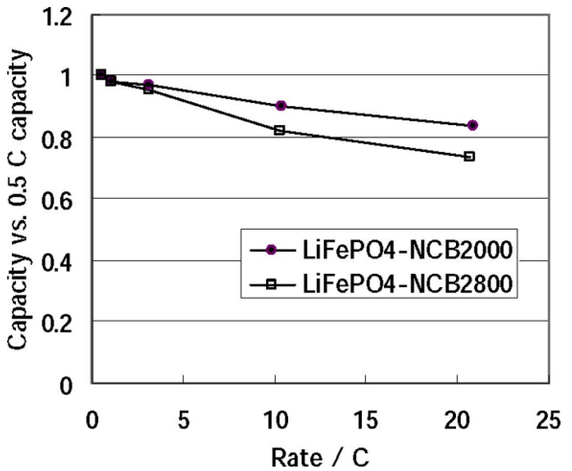

Figure 8. (Color online) Discharge rate performance of heat-treated CNBs (counter electrode: $LiFePO_4$).

carbon. In 2000 and 1500°C, the plateau was also observed. These results indicate that graphitization which causes specific electrolyte decomposition occurred above 1500°C.

Figure 6 shows the relationship between temperature of heat-treatment and initial irreversible capacity. The difference between 1200 and 1500°C was large. The difference of irreversible capacity between 1200 and 1500°C is correlated to the amount of hydrogen. The relationship of irreversible capacity and the amount of hydrogen has been reported.[22,23] The more the hydrogen is, the more the irreversible capacity is. The irreversible capacity in 2000°C was lower than in 2800°C while the amount of hydrogen in 2000°C was lower than in 2800°C. Compared to 1500 and 2800°C, the irreversible capacity in 1500°C is lower than in 2800°C while the amount of hydrogen in 2800°C was lower than in 1500°C. The irreversible capacity for 2800°C was larger than for 1500°C. This irreversible capacity is caused by the large plateau at 0.8 V, which is ascribed to electrolyte decomposition.

The relation between the C rate and discharge capacity is shown in Fig. 7. The discharge capacity of 2800°C decreased at 15C; however the discharge capacity of 2000°C was larger than 2800°C above 15C. The 1500, 1200, and 1000°C showed much lower performance.

The reason for the superior discharge rate of 2000°C is assumed that lithium-ion deintercalation is affected by the surface of carbon particles.

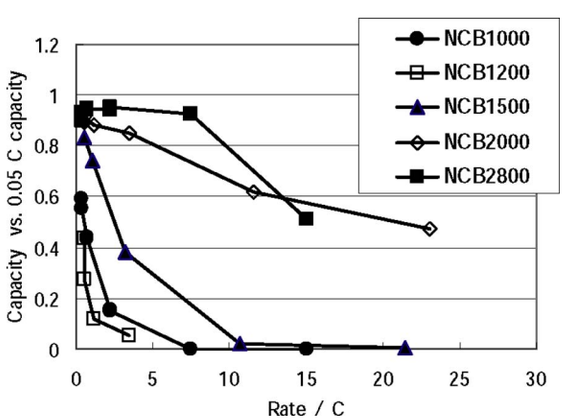

Figure 7. (Color online) Discharge rate performance of heat-treated CNBs (counter electrode: Li metal).

CNBs heat-treated at 2000 and 2800°C have almost the same BET surface area. However, the conditions of edge planes are different because the more graphitized structure has a more basal plane. It was analyzed by XRD and Raman spectroscopy. As discussed in Fig. 4, 2000°C CNBs has the smallest amorphous region on the surface. The amorphous region on the surface of CNBs affects the discharge rate ability.

We investigated the discharge rate performance of 2000 and 2800°C using $LiFePO_4$ as the counter electrode in Fig. 8. The capacity of the $LiFePO_4$ counter electrode is more than twice that of the working electrode because sufficient capacity of the counter electrode can decrease the effect of the counter electrode in measuring the performance of the working electrode. The discharge capacity of 2000°C CNBs was larger than that of 2800°C CNBs at a high rate. This tendency is nearly the same, as shown in Fig. 7.

Figure 9 shows the Nyquist plot of CNBs using a three-electrode cell containing lithium metal counter and reference electrodes. The potential of the CNB electrode was stepped from open-circuit voltage to 1.0, 0.8, 0.6, 0.4, 0.2, and 0.1 V and kept at each potential for enough time to reach steady state. CNBs heat-treated at 2800, 2000, and 1500°C at 1.0 V show a semicircle in high frequency from about 10 kHz to 10 Hz. This semicircle is ascribed to surface film resistance on the carbon negative electrode.[24] At a low frequency, 1500°C showed the same semicircle, while 2000 and 2800°C rose vertically. This low frequency semicircle is ascribed to charge-transfer resistance. Thus it appears that lithium ions can intercalate at 1.0 V in 1500°C CNBs. Lithium ions cannot intercalate into 2800 and 2000°C CNBs at 1.0 V. At 0.8 V the characteristic semicircle at low frequency was smaller than that for 1.0 V in all CNBs. At 0.6 V two semicircles were clearly observed in 2000°C. At 0.2 V two semicircles were observed in 2800°C. These results indicate that the lithium-ion intercalation occurs at around 1.0 V in 1500°C, around 0.6 V in 2000°C, and around 0.2 V in 2800°C. These results agree with the charge/discharge curves in Fig. 5. At 0.1 V the semicircles for 2000 and 2800°C are almost identical, while the semicircle for 1500°C was larger than that for 2000 and 2800°C. However, the semicircle for 2000°C was smaller over a wider potential range than for the 2800 and 1500°C. The charge-transfer resistance in 2000°C CNBs was smaller than that of 1500 and 2800°C CNBs in the range of 0.1–0.4 V. It indicates the higher discharge ability in 2000°C CNBs.

Figure 10 shows the results of DSC measurement of CNBs. A small peak exists at around 130°C and a large peak exists between 200 and 300°C. The peak at 130°C has been reported as the decomposition of SEI, and the heat generation at 130°C is proportional to the surface area of carbon.[13-17] In this study the heat generation at

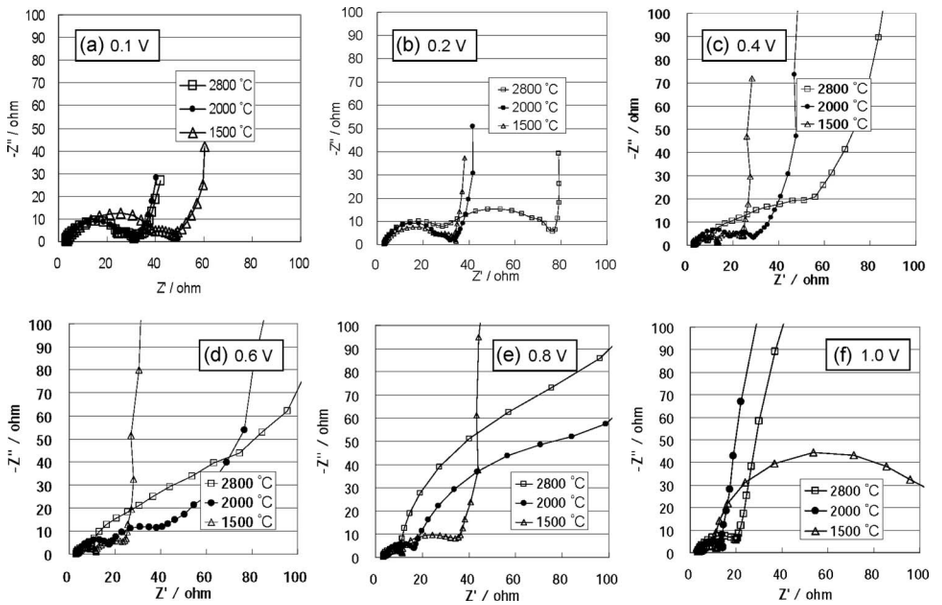

Figure 9. Nyquist plot of the heat-treated CNB electrode in 1 M $LiPF_6$/EC + DEC (3:7) at (a) 0.1, (b) 0.2, (c) 0.4, (d) 0.6, (e) 0.8, and (f) 1.0 V.

130°C was not much different among the samples. This result indicates the same BET surface area among the various CNBs.

The lower the temperature of heat-treatment is, the higher the temperature of the exothermic peak is. The temperature of the peak is on the order of 1000 < 1500 < 2000 < 2800°C. The temperature of the largest exothermic peak is proportional to the temperature of the heat-treatment of CNBs.

The largest peak is most likely the reaction of lithiated carbon and electrolyte or binder.[13-17] If the largest peak was the reaction of lithiated carbon, the heat generation should be proportional to the charge capacity. Figure 11 shows the relationship between charge capacity and the amount of heat generation at the largest peak. There is a nonlinear relationship. This is due to neglecting the potential of Li-GIC. Instead of charge capacity, charged energy can be used as the parameter (Fig. 12). The charged energy was calculated by the integral of charge curves in the range of 0.005–1.0 V. This result shows a linear relationship. These results suggest that the amount of heat generation at the largest peak is proportional to the energy of the lithiated carbon. From the results of Fig. 10 and 12, the CNBs heat-treated in a higher temperature were easier to be exothermized in an abuse condition. The temperature of 2000°C is safest in the point of heat flow because of the lowest energy storage among heat-treated CNBs.

Conclusion

We investigated the physical properties and electrochemical characteristics of heat-treated CNBs. Initial irreversible capacity was minimized in CNBs heat-treated at 2000°C. The 2000°C CNBs contained the lowest amorphous region by Raman spectroscopy. High rate discharge ability was highest in 2000°C CNBs. The result of alternative impedance spectrometry showed that the charge-transfer resistance of 2000°C CNB was smaller over a wide potential range.

From the results of DSC measurement, the higher the temperature of heat-treatment is, the lower the temperature of the exothermic peak is. The amount of exothermal reaction was proportional to the energy stored in the lithiated CNBs.

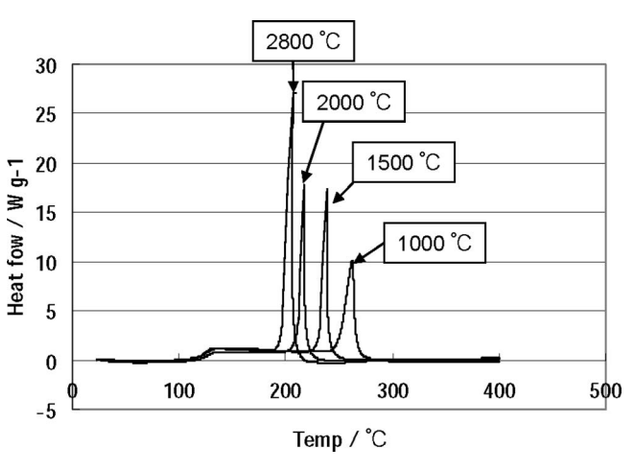

Figure 10. DSC of fully charged heat-treated CNBs.

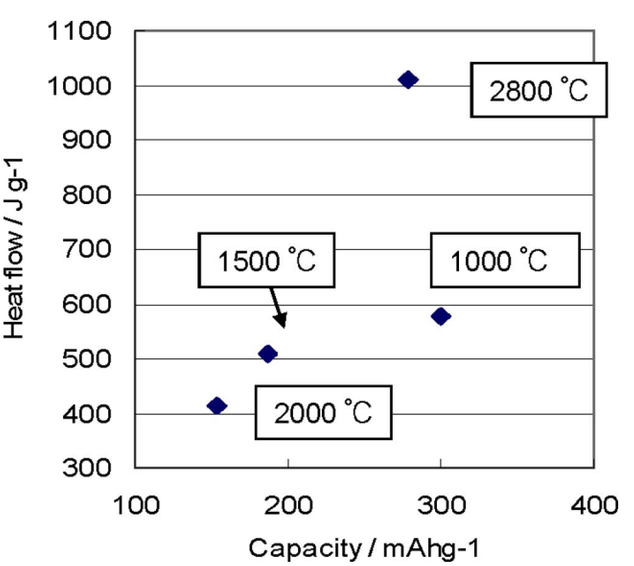

Figure 11. (Color online) Relationship between discharge capacity and heat flow at maximum peak.

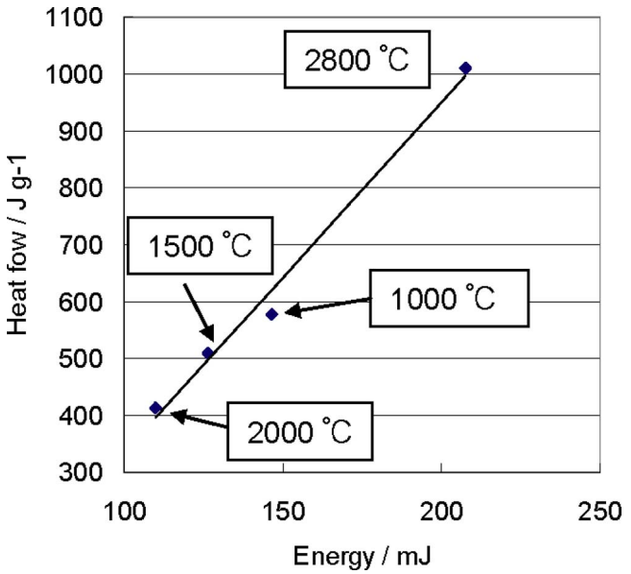

Figure 12. (Color online) Relationship between heat flow at maximum peak and discharge capacity energy below 1.0 V.

TDK Corporation assisted in meeting the publication costs of this article.

References

1. A. Funabiki, M. Inaba, Z. Ogumi, S. Yuasa, J. Otsuli, and A. Tasaka, *J. Electrochem. Soc.*, **145**, 172 (1998).
2. A. Funabiki, M. Inaba, T. Abe, and Z. Ogumi, *Electrochim. Acta*, **45**, 865 (1999).
3. F. Disma, L. Aymard, L. Dupont, and J.-M. Tarascon, *J. Electrochem. Soc.*, **143**, 3959 (1996).
4. F. Salver-Disma, C. Lenain, B. Beaudoin, L. Aymard, and J.-M. Tarascon, *Solid State Ionics*, **98**, 145 (1997).
5. Q. Wang, H. Li, L. Chen, X. Huang, D. Zhong, and E. Wang, *J. Electrochem. Soc.*, **150**, A1281 (2003).
6. A. Odani, A. Nimberger, B. Markovsky, E. Sominski, E. Levi, V. G. Kumar, M. Motiei, A. Gedanken, P. Dan, and D. Aurbach, *J. Power Sources*, **119–121**, 517 (2003).
7. N. Li, D. T. Mitchell, K. P. Lee, and C. R. Martin, *J. Electrochem. Soc.*, **150**, A979 (2003).
8. K. Honda, M. Yoshimura, K. Kawakita, A. Fujishima, Y. Sakamoto, K. Yasui, N. Nishio, and H. Masuda, *J. Electrochem. Soc.*, **151**, A532 (2004).
9. J. Hu, H. Li, and X. Huang, *Solid State Ionics*, **178**, 265 (2007).
10. H. Wang, T. Abe, S. Maruyama, Y. Iriyama, Z. Ogumi, and K. Yoshikawa, *Adv. Mater. (Weinheim, Ger.)*, **17**, 2857 (2005).
11. H. Buqa, D. Goers, M. Holzapfel, M. E. Spahr, and P. Novák, *J. Electrochem. Soc.*, **152**, A474 (2005).
12. B. Markovsky, M. D. Levi, and D. Aurbach, *Electrochim. Acta*, **43**, 2287 (1998).
13. M. D. Levi and D. Aurbach, *J. Phys. Chem. B*, **101**, 4641 (1997).
14. J. S. Gnanaraj, M. D. Levi, E. Levi, G. Salitra, D. Aurbach, J. E. Fischer, and A. Claye, *J. Electrochem. Soc.*, **148**, A525 (2001).
15. A. Du Pasquier, F. Disma, T. Bowmer, A. S. Gozdz, G. Amatucci, and J.-M. Tarascon, *J. Electrochem. Soc.*, **145**, 472 (1998).
16. E. P. Roth, D. H. Doughty, and J. Franklin, *J. Power Sources*, **134**, 222 (2004).
17. H. Maleki, G. Deng, I. Kerzhner-Haller, A. Anani, and J. N. Howard, *J. Electrochem. Soc.*, **147**, 4470 (2000).
18. J. Yamaki, H. Takatsuji, T. Kawamura, and M. Egashira, *Solid State Ionics*, **148**, 241 (2002).
19. M. N. Richard and J. R. Dahn, *J. Electrochem. Soc.*, **146**, 2068 (1999).
20. J. R. Dahn, F. Fong, and M. J. Spoon, *Phys. Rev. B*, **42**, 6424 (1990).
21. T. Zheng, J. N. Reimers, and J. R. Dahn, *Phys. Rev. B*, **51**, 734 (1995).
22. K. Tatsumi, T. Akai, T. Imamura, K. Zaghib, N. Iwashita, S. Higuchi, and Y. Sawada, *J. Electrochem. Soc.*, **143**, 1923 (1996).
23. Y. Yamamoto, T. Tahara, and R. Harada, Japanese Pat. 2003-1803 (2003).
24. A. Hartschuh, H. N. Pedrosa, L. Novotny, and T. D. Krauss, *Science*, **301**, 1354 (2003).
25. J. O. Besenhard, M. Winter, J. Yang, and W. Biberacher, *J. Power Sources*, **54**, 228 (1995).